

Manuscript version: Author's Accepted Manuscript

The version presented in WRAP is the author's accepted manuscript and may differ from the published version or Version of Record.

Persistent WRAP URL:

<http://wrap.warwick.ac.uk/134781>

How to cite:

Please refer to published version for the most recent bibliographic citation information. If a published version is known of, the repository item page linked to above, will contain details on accessing it.

Copyright and reuse:

The Warwick Research Archive Portal (WRAP) makes this work by researchers of the University of Warwick available open access under the following conditions.

Copyright © and all moral rights to the version of the paper presented here belong to the individual author(s) and/or other copyright owners. To the extent reasonable and practicable the material made available in WRAP has been checked for eligibility before being made available.

Copies of full items can be used for personal research or study, educational, or not-for-profit purposes without prior permission or charge. Provided that the authors, title and full bibliographic details are credited, a hyperlink and/or URL is given for the original metadata page and the content is not changed in any way.

Publisher's statement:

Please refer to the repository item page, publisher's statement section, for further information.

For more information, please contact the WRAP Team at: wrap@warwick.ac.uk.

Signal Estimation in Cognitive Satellite Networks for Satellite-Based Industrial Internet of Things

Mingqian Liu, *Member, IEEE*, Nan Qu, Jie Tang, *Senior Member, IEEE*, Yunfei Chen, *Senior Member, IEEE*, Hao Song, and Fengkui Gong, *Member, IEEE*

Abstract—Satellite Industrial Internet of Things (IIoT) plays an important role in industrial manufactures without requiring the support of terrestrial infrastructures. However, due to the scarcity of spectrum resources, existing satellite frequency bands cannot satisfy the demand of IIoT, which have to explore other available spectrum resources. Cognitive satellite networks (CSNs) are promising technologies and have the potential to alleviate the shortage of spectrum resources and enhance spectrum efficiency by sharing both spectral and spatial degrees of freedom. For effective signal estimations, multiple features of wireless signals are needed at receivers, the transmissions of which may cause considerable overhead. To mitigate the overhead, part of parameters, such as modulation order, constellation type, signal to noise ratio (SNR), could be obtained at receivers through signal estimation rather than transmissions from transmitters to receivers. In this paper, a grid method is utilized to process the constellation map to obtain its equivalent probability density function. Then, binary feature matrix of the probability density function is employed to construct a cost function to estimate the modulation order and constellation type for multiple quadrature amplitude modulation (MQAM) signal. Finally, an improved M_2M_∞ method is adopted to realize the SNR estimation of MQAM. Simulation results show that the proposed method is able to accurately estimate the modulation order, constellation type and SNR of MQAM signal, and these features are extremely useful in satellite-based IIoT.

Index Terms—Industrial Internet of Things, cognitive satellite networks, modulation order estimation, constellation type estimation, signal to noise ratio estimation

I. INTRODUCTION

Satellite industrial Internet of Things (IIoT) possesses many appealing attributes, including wide-area coverage, long-distance transmissions, and remote-area information collections, compared to traditional ground IIoT [1]. Recently,

This work was supported in part by the National Natural Science Foundation of China under Grant 61501348 and Grant 61801363, in part by the Shaanxi Provincial Key Research and Development Program Grant 2019GY-043, in part by the Joint Fund of Ministry of Education of the People's Republic of China under Grant 6141A02022338, in part by the China Postdoctoral Science Foundation under Grant 2017M611912, in part by the 111 Project under Grant B08038, and in part by the China Scholarship Council under Grant 201806965031. (*Corresponding author: Jie Tang.*)

M. Liu, N. Qu and F. Gong are with the State Key Laboratory of Integrated Service Networks, Xidian University, Shaanxi, Xi'an 710071, China (e-mail: liu@mail.xidian.edu.cn; nqu@stu.xidian.edu.cn; fkgong@xidian.edu.cn).

J. Tang is with the school of Electronic and Information Engineering, South China University of Technology, Guangzhou 510641, China. (e-mail: cejtang@scut.edu.cn)

Y. Chen is with the School of Engineering, University of Warwick, Coventry, West Midlands United Kingdom of Great Britain and Northern Ireland CV4 7AL (e-mail: Yunfei.Chen@warwick.ac.uk)

H. Song is with the Bradley Department of Electrical and Computer Engineering, Virginia Tech, Blacksburg 24060, VA, USA (e-mail: haosong@vt.edu).

with the rapid development of wireless and mobile technologies, the conflict between the explosive growth and the scarcity of spectrum resources has become more and more serious [2]-[4]. As a precious and costly resource, the licenses of which are granted by governments. Therefore, it is challenging for satellite IIoT to obtain an adequate licensed spectrum to meet the demand of broadband satellite services [5]-[8]. To cope with that, cognitive satellite networks (CSNs), as a potential solution, have been developed for the effective utilization of unlicensed bands and sharing spectrum resources with other wireless systems, like terrestrial cellular networks [9]. The spectrum access opportunities for secondary users are supposed to be assured within the bearable interference level of the primary user [10]. The main problem to guarantee the quality of service (QoS) of CSNs is to handle the interference across two networks. Thus, the signal estimation of both primary user and secondary user is vital for CSNs.

Multiple quadrature amplitude modulation (MQAM) signals have many advantages, such as high spectrum efficiency and strong noise tolerance, which can be used in satellite communications to achieve high transmission efficiency without increasing bandwidth resources [11]. Thus, the second-generation satellite digital video broadcasting (DVB-S2) has already increased the optional modulation order to 16 and 32 [12]. Moreover, 16QAM and 16APSK modulations are also recommended in DVB-SH [13]. China's digital TV terrestrial broadcasting system even uses higher-order modulations such as 16QAM, 32QAM, and 64QAM. As a specialized and novel modulation method, MQAM signals have derived many new constellation types. For example, the United States Department of Defense proposed a constellation mapping of circular QAM modulation in Appendix D of the military standard MIL-STD-188-110C issued at the end of 2011, referred to as 110C [14]. In 2016, Farbod Kayha proposed a circular constellation QCI [15], which is mapped by a square constellation.

For the effective demodulation and decoding of MQAM signals, some signal parameters are required, including modulation order, constellation type, and signal to noise ratio (SNR) [16]-[17]. Some of these modulation parameters could be obtained through the feedback from transmitters. The transmissions of these parameters may cause severe overhead, and dedicated control channels need to be reserved and designed for these parameter transmissions. Hence, estimating signal parameters at the receiver side would be a more realistic and applicable way [18]. Unfortunately, as a complicated modulation method, signal estimations of the MQAM signal are very challenging. Furthermore, for preferred modulation

performance, the accuracy of signal estimations is critical, as estimated parameters directly determine the selection of demodulation algorithms. Therefore, in this paper, we focus on exploring the non-data assisted estimation methods of the aforementioned signal parameters for MQAM signals in CSNs.

Due to the benefit of no training data needed to sent from transmitters, on-data assisted estimations are more suitable for batch transmission of data. Some research achievements have been published for non-data assisted signal estimations. The authors in [19] used nuclear density estimation to identify square 4/16/64QAM signals. High-order cumulants and signal cyclostationarity are proposed for 4/16/64QAM signal estimations in [20]. The authors in [21] converted the time-frequency of the Wigner-Ville distribution (WVD) into an incoming signal to calculate the complexity metric of the signal, Renyi entropy, based on which the Dempster-Shafer theory is used to estimate the signal. A high-order cumulant-based estimation method is introduced in [22] to recognize the 16/64QAM signals. In [23], the constellation diagram is used to detect MQAM signals. Notably, most recent work on MQAM signals is limited to square or cross-shaped QAM signals, which may incur the fact that these methods may not be able to work out in 110C and QCI circular QAM signals. Moreover, there is still no work done on constellation type estimations. The existing SNR estimation methods for MQAM signals with constellation type of square and cross are based on the knowledge of modulation order and constellation type. The authors in [24] proposed a time-varying autocorrelation function (TVAF) to estimate SNR. In [25], an improved vector error method is put forward to estimate SNR of 4QAM signals. In [26], the M_2M_∞ method is employed to generate new monotonic statistics, combined with the look-up table method to estimate SNR for the square constellation MQAM signals. The authors in [27] proposed an improved SNR estimation method to achieve robust adaptive beamforming. However, these SNR estimation methods cannot be applicable for all types of constellations, which require prior information, such as the modulation order and the constellation type.

In this paper, to mitigate the overhead, a novel non-data method is proposed using a grid method and binary feature matrix to estimate modulation order, constellation type, and SNR in CSNs for satellite-based IIoT. The main creative contributions of this paper can be summarized as follows:

- According to any received signal sequences, the probability density function of the constellation points is estimated by the introduced grid method.
- The cross section and the peak proportional coefficient are employed to obtain the binary characteristic matrix of the probability density function for further process.
- Based on estimated parameters, the cost function is defined to estimate the constellation type, which contains both modulation order and constellation type.
- SNR is estimated by using the improved M_2M_∞ method and the look-up table method.

The rest of this paper is organized as follows. The system model considered in this paper is presented in Section II. The modulation order and the constellation type estimation method

is proposed in Section III. In Section IV, a SNR estimation method is introduced. Section V shows the numerical results to verify the estimation performance. Finally, Section VI concludes the whole paper.

II. SYSTEM MODEL

An uplink cognitive satellite terrestrial network used in IIoT is considered, where the terrestrial network shares the spectrum with the satellite network [9]. Let $q(t)$ denote received signals in CSN for satellite-based IIoT, which is given by

$$q(t) = \sum c(t) h(t - nT_s) + n(t), \quad (1)$$

where $n(t)$ represents additive white Gaussian noise with a bilateral power spectral density of $\sigma_0/2$, $h(t - nT_s)$ denotes a single baseband waveform with a width of T_s . $c(t)$ is the MQAM signal, which is expressed as

$$c(t) = \sum_n A_n \cos(\omega_c t + \varphi_n), \quad (2)$$

where A_n is the amplitude of baseband signal. The orthogonal representation of the MQAM signal is

$$c(t) = \sum_n A_n \cos \varphi_n \cos \omega_c t + \sum_n A_n \sin \varphi_n \sin \omega_c t. \quad (3)$$

Assuming that

$$\begin{cases} X_n = A_n \cos \varphi_n, \\ Y_n = A_n \sin \varphi_n, \end{cases} \quad (4)$$

so (3) can be rewritten as

$$\begin{aligned} c(t) &= \sum_n X_n \cos \omega_c t + \sum_n Y_n \sin \omega_c t \\ &= I_M \cos \omega_c t + Q_M \sin \omega_c t, \end{aligned} \quad (5)$$

where M represents the modulation order, I_M and Q_M are the Amplitude on its in-phase and quadrature components, respectively, and its value range is $\{\pm a(2i+1) | i = 0, 1, \dots, K\}$, a denotes the amplitude factor. The constellation diagram represents the distribution of the end points of the signal vector, which can be used to visually represent the multi-digit digital modulated signal. For MQAM signal, the coordinates of the constellation point on the complex plane are (I_M, Q_M) . $K = \log_2(M/4)$ in square and cross-shaped MQAM signal in a constellation diagram, and there is no constellation point at the vertices of the square outline in the cross-shaped constellation.

The 110C-MQAM modulation uses a circular constellation mapping to achieve a better peak-to-average ratio without sacrificing the pseudo-Gray code characteristics of the square constellation. Meanwhile, the number of modulus values of the constellation corresponding to QCI-MQAM modulation is relatively small, which can better resist nonlinear distortion in satellite communication.

III. MODULATION ORDER AND CONSTELLATION TYPE ESTIMATION OF MQAM FOR SATELLITE-BASED IIOT

A. Probability Density Function Estimation of Constellation Points

The reconstruction of the constellation is based on the recovered baseband signal, which can be expressed as

$$r(t) = q(t) \otimes h^*(-t) = \sqrt{S}s(t) + \sqrt{N}n'(t), \quad (6)$$

where \otimes represents convolution, S is the signal power, and N is the noise power. $s(t) = \sum c(t)h'(t - nT_s)$, $h'(t) = h(t) \otimes h^*(-t)$ is raised cosine function. and $n'(t) = n(t) \otimes h^*(-t)$ is the noise element. Suppose the coordinates of each constellation point in the received sequence are (r_{iI1}, r_{iQ1}) , $i = 1, 2, \dots, L$, where L represents the number of constellation points received. The power normalization factor of the constellation point is

$$P_{Norm} = \sqrt{\frac{\sum_{i=1}^L (r_{iI1}^2 + r_{iQ1}^2)}{L}}, \quad (7)$$

so the power normalized constellation point coordinate is $(r_{iI2}, r_{iQ2}) = \left(\frac{r_{iI1}}{P_{Norm}}, \frac{r_{iQ1}}{P_{Norm}}\right)$. The average power of constellation points is $P_{QAM} = 1$. According to the definition of SNR, the SNR of the received signal can be expressed as

$$SNR = \frac{S}{N} = \frac{P_{QAM}}{2\sigma_0^2} = \frac{1}{2\sigma_0^2}, \quad (8)$$

where σ_0 denotes the unilateral power spectral density of Gaussian noise.

Set the origin to coordinate correction, we can get the origin coordinates

$$O(o_x, o_y) = O\left(\frac{1}{L} \sum_{i=1}^L r_{iI2}, \frac{1}{L} \sum_{i=1}^L r_{iQ2}\right). \quad (9)$$

The coordinates of the constellation points after coordinate correction are $r_i(r_{iI}, r_{iQ})$, $r_{iI} = r_{iI2} - o_x$, $r_{iQ} = r_{iQ2} - o_y$, where $i = 1, 2, \dots, L$. The i -th constellation point after power normalization and coordinate correction $r_i(r_{iI}, r_{iQ})$ can be expressed as

$$r_i = s_i + v_i, i = 1, 2, \dots, L, \quad (10)$$

where s_i is the constellation point sent by the sender, and its coordinates are (x_k, y_k) . v_i denotes the effect of additive white Gaussian noise on the constellation. L represents the number of constellation points received.

The probability density function of the MQAM signal constellation is a continuous function, and the received signal constellation is discrete. The probability density function can be obtained by continuing discrete points. Assuming that the received signal is long enough, the probability density function of the MQAM signal can be estimated using the grid method. The coordinates of the signal constellation point r_i is (r_{iI}, r_{iQ}) , the length of the received signal is L . Construct a square grid whose x -axis and y -axis are both set from $-r_I$ to r_I , where $r_I = \max(|r_{iI}|, |r_{iQ}|)$. Define the mesh density $Meshnum$ as the number of meshes divided

in a single direction, that is, the mesh map divided in the $Meshnum * Meshnum$ determined area, each mesh size is

$$Meshsize = \frac{2r_I}{Meshnum}. \quad (11)$$

The mesh is equivalent to the xoy coordinate plane, and the coordinates in the coordinate plane can be expressed as , then the function value of each point in the plane is

$$g(x_p, y_p) = \frac{1}{L} \sum_{\substack{r'_{iI} \in (x_p, x_p + Meshsize) \\ r'_{iQ} \in (y_p, y_p + Meshsize)}} 1. \quad (12)$$

For a constellation points series $r_i(r_{iI}, r_{iQ})$ where $i = 1, 2, \dots, L$, the continuous probability density function can be estimated with

$$g(x, y) = \sum_{p=1}^{Meshnum^2} g(x_p, y_p). \quad (13)$$

where $g(x_p, y_p)$ is constructed with (12).

Using the grid method to estimate the probability density function of constellation points, the key part is the selection of grid density. The larger the matrix of the estimated probability density function is, the higher the complexity of the subsequent algorithm is. If the mesh density is too small, the resolution will be too low, which will cause the probability density function estimation value to not characterize the constellation of the modulation order too large, resulting in estimate errors. Since the number of received constellation points is limited, the accuracy of the estimated probability density function is limited. It is known from the law of large numbers that when the number of constellation points approaches infinity, the probability density function estimated from continuous discrete points will infinitely approach the probability density function of the standard constellation diagram. By knowing the geometric distribution of the constellation diagram, each constellation point in any constellation type is symmetric about the x-axis, the y-axis, and the origin. In this paper, a data reuse method is adopted to estimate the probability density function in a more accurate way. When the coordinates of a certain constellation point (r_{iI}, r_{iQ}) is obtained after the coordinate correction, its mirror image multiplexed data coordinates are $(-r_{iI}, r_{iQ})$, $(r_{iI}, -r_{iQ})$ and $(-r_{iI}, -r_{iQ})$.

B. Feature Extraction based on Constellation Points Probability Density Function

After estimating the probability density function of the constellation point, the probability density function graph is processed to obtain a binary matrix that can characterize the modulation order of the signal and the constellation type. It is divided into two steps: 1) the determination of the grid theory boundary; 2) the acquisition of the binary feature matrix of the probability density function.

1) *Determination of the Grid Theory Boundary*: First, this paper assumes that the probability density function of the received signal points conforms to the two-dimensional Gaussian mixture model. Under the one-dimensional normal curve, the

area of a certain interval on the horizontal axis reflects the percentage of the number of cases in the interval as a percentage of the total number of cases, that is, the probability that the variable value falls within the interval. In probability theory, we refer to an event with a probability close to zero as a small probability event, indicating that it occurs very frequently in a large number of repeated experiments. In a one-dimensional normal distribution $f'(x) = \frac{1}{\sqrt{2\pi\sigma_0^2}} \exp\left\{-\frac{(x-\mu)^2}{2\sigma_0^2}\right\}$, the probability of x falling outside $(\mu - 3\sigma, \mu + 3\sigma)$ is less than 3×10^{-5} . In practice, it is often believed that the corresponding event will not happen. Basically, the interval can be regarded as the actual value range of the random variable. This is called the "3 σ " principle of normal distribution.

In a two-dimensional normal distribution, the volume under the surface reflects the probability that the variable value falls within the interval, which can be expressed as

$$f'(x, y) = \frac{1}{2\pi\sigma_0^2} \exp\left\{-\frac{(x-x_0)^2 + (y-y_0)^2}{2\sigma_0^2}\right\}, \quad (14)$$

where (x_0, y_0) represents the center of the circle, r denotes the radius, and the volume covered under the surface is

$$V(r) = \int_0^r dV = 1 - \exp\left\{-\frac{r^2}{2\sigma_0^2}\right\}. \quad (15)$$

In this paper, when the probability is less than ε , the corresponding event will not occur in the actual problem. Let $V(r_0) = 1 - \varepsilon$, the grid theory boundary determination is

$$\begin{cases} map_{\min} = \min_{k=1,2,\dots,M} (x_k, y_k) - \sigma_0\sqrt{-2\ln\varepsilon}, \\ map_{\max} = \max_{k=1,2,\dots,M} (x_k, y_k) + \sigma_0\sqrt{-2\ln\varepsilon}, \end{cases} \quad (16)$$

where (x_k, y_k) represents the coordinates of the k -th transmitted constellation point.

2) *Binary Feature Matrix of Probability Density Function:* Assuming that the probability density function of the received signal points conforms to the two-dimensional Gaussian mixture model, the probability density function of all constellation points is expressed as

$$f(x, y) = \sum_{k=1}^M \pi_k f_k(x, y), \quad (17)$$

where M represents the modulation order, $f_k(x, y) = \frac{1}{2\pi\sigma_0^2} \exp\left\{-\frac{(x-x_k)^2 + (y-y_k)^2}{2\sigma_0^2}\right\}$, and (x_k, y_k) denotes the coordinates of the k -th transmission constellation point. Assume that each constellation point has the same probability of emission, then $\pi_k = \frac{1}{M}$, $k = 1, 2, \dots, M$.

As shown in Fig. 1, when the SNR is not too low, the probability density function of the constellation point should have M local peaks. Each peak consists of two parts, one is the peak of the probability density function corresponding to the constellation point, and the other part is the trailing superposition of the probability density function corresponding to the remaining points. The local peak can be expressed as

$$F_{\max} = \frac{1 + \sum_{i=1, i \neq k}^M \exp\left\{-\frac{(x_i-x_k)^2 + (y_i-y_k)^2}{2\sigma_0^2}\right\}}{M2\pi\sigma_0^2}. \quad (18)$$

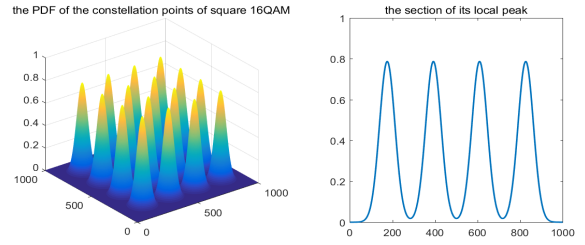


Fig. 1. The probability density function of the constellation point of square 16QAM and the section of its local peak

In order to estimate the number of local peaks and constellation type by using the probability density function, a certain section $f(x, y) = pF_{\max}$ is used to characterize the constellation type, where p is the peak scale factor. And the binary real points can be obtained by

$$g(b_{xi}, b_{yi}) \geq f(x, y). \quad (19)$$

When the transmit power is constant, taking a fixed ε , as the SNR increases, $\sigma_0\sqrt{-2\ln\varepsilon}$ decreases. That is, for a certain transmission constellation point, the probability density function of other transmitting constellation points has a function value of approximately 0 at this point. The section can be approximated by M circles and M is the modulation order. Each circle is centered on the sending constellation point, and its radius can be expressed as

$$r = \sqrt{-2\sigma_0^2 \ln(2\pi M\sigma_0^2 p F_{\max})}. \quad (20)$$

Therefore, the binary feature matrix is extracted after obtaining the probability density function by the grid method, and the theoretical value of the true value points is

$$BinVal = Meshnum^2 * \eta, \quad (21)$$

where $Meshnum$ denotes the mesh density and η is the true value scale factor, which is expressed as

$$\eta = \frac{\pi [-2\sigma_0^2 \ln(2\pi M\sigma_0^2 p F_{\max})]}{(map_{\max} - map_{\min})^2}. \quad (22)$$

C. Modulation Order and Constellation Type Estimation Based on Subtractive Clustering

1) *Clustering Algorithm and Cost Function:* The N_b truth point coordinates in the binary real points are expressed as $B_i(b_{xi}, b_{yi})$, $i = 1, 2, \dots, N_b$. The binary clusters are subjected to subtractive clustering under different clustering radii $r_{k'}$, and cluster centers at different cluster radii are obtained, which can be expressed as $(bx_{k',i}, by_{k',i})$, $i = 1, 2, \dots, N_b$, $k' = 1, 2, \dots, 5$. Coordinate correction and power normalization are performed on the cluster centers obtained by different clustering algorithms to obtain a new cluster center coordinate $(x_{k',i}, y_{k',i})$, $i = 1, 2, \dots, N_b$, $k' = 1, 2, \dots, 5$, where

$$\begin{cases} x'_{k',i} = bx_{k',i} - \frac{1}{N_b} \sum_{i=1}^{N_b} bx_{k',i}, \\ y'_{k',i} = by_{k',i} - \frac{1}{N_b} \sum_{i=1}^{N_b} by_{k',i}, \end{cases} \quad (23)$$

$$\begin{cases} x_{k',i} = \frac{x'_{k',i}}{\sqrt{x'_{k',i}{}^2 + y'_{k',i}{}^2}}, \\ y_{k',i} = \frac{y'_{k',i}}{\sqrt{x'_{k',i}{}^2 + y'_{k',i}{}^2}}. \end{cases} \quad (24)$$

Define the cost function of the constellation type estimation for MQAM as

$$J_{k,p} = \frac{Ja_{k,p}}{\max_p Ja_{k,p}} + \frac{Jb_{k,p}}{\max_p Jb_{k,p}}, \quad (25)$$

where $k = 1, 2, \dots, 5$, $p = 1, 2, \dots, 14$. $J_{k,p}$ denotes the degree of similarity between the cluster center obtained by the k -th cluster radius and the p -th standard constellation map of the constellation, which are expressed as following

$$Ja_{k',k} = \begin{cases} \sum_{i=1}^{N_b} \min \left(\sqrt{(x_{k',i} - x'_{k,j})^2 + (y_{k',i} - y'_{k,j})^2} \right), & M \leq N_b \\ \sum_{j=1}^M \min \left(\sqrt{(x_{k',i} - x'_{k,j})^2 + (y_{k',i} - y'_{k,j})^2} \right), & M > N_b \end{cases} \quad (26)$$

$$Jb_{k',k} = \begin{cases} \frac{1}{M} \sum_{i=1}^{N_b} \min \left(\sqrt{(x_{k',i} - x'_{k,j})^2 + (y_{k',i} - y'_{k,j})^2} \right), & M \leq N_b \\ \frac{1}{N_b} \sum_{j=1}^M \min \left(\sqrt{(x_{k',i} - x'_{k,j})^2 + (y_{k',i} - y'_{k,j})^2} \right), & M > N_b \end{cases} \quad (27)$$

where $(x''_{p,j}, y''_{p,j})$ is the standard constellation diagram after power normalization, $p = 1, 2, \dots, 14$ represent the constellations of 4QAM, 16QAM-square, 16QAM-110C circular, 16QAM-QCI circular, 32QAM-cross, 32QAM-110C circular, 32QAM-QCI circular, 64QAM-square, 64QAM-110C circular, 64QAM-QCI circular, 128QAM-cross, 256QAM-square, 256QAM-110C circular, 256QAM-QCI circular, respectively. $j = 1, 2, \dots, M$ denotes the corresponding modulation order. $(x_{k,i}, y_{k,i})$ is the power normalization result of the cluster center obtained by the k -th cluster radius of the to-be-identified constellation, $i = 1, 2, \dots, N_b$, $k' = 1, 2, \dots, 5$.

Define the constellation type estimation cost function as $J_{k',k}$, the constellation type estimation problem can be formulated as

$$k^* = \arg \min_{k'=1,2,\dots,5} J_{k',k}, \quad (28)$$

where k^* is the parameter that takes $J_{k',k}$ to the minimum value.

Note that both the modulation order and the constellation type can be estimated by (28) at the same time. In the construction process of the cost function, both $Ja_{k,p}$ and $Jb_{k,p}$ can measure the similarity between the clustering center of the constellation to be identified at the k -th cluster radius and the p -th standard constellation. However, when k is small, the cluster radius is large, $Ja_{k,p}$ will take the minimum value when p is small. Using $Ja_{k,p}$ as a cost function alone, high-order QAM is easily misjudged as 4/16QAM at high SNR. When k is larger, the cluster radius is smaller, and $Jb_{k,p}$

TABLE I
AVERAGE SNR CORRESPONDING TO BER $\leq 10^{-5}$

User data rate(bps)	Modulation	Average SNR (dB)
12800	256QAM	27
11200	128QAM	24
9600	64QAM	21
8000	32QAM	19
6400	16QAM	16
3200	4QAM	9

will take the minimum value when p is larger. Using $Jb_{k,p}$ alone as a cost function, low-order QAM is easily misjudged as 256QAM at low SNR. Therefore, after normalizing $Ja_{k,p}$ and $Jb_{k,p}$ in this paper, the new cost function is obtained by merging them with equal weights.

2) *Parameter Selection*: In the communication system, the bit error rate is required, and the maximum bit error rate cannot exceed a certain specific index. The user data rate is specified in Appendix C of the military standard MIL-STD-188-110C. Meanwhile, it is stipulated that under the additive white Gaussian noise (AWGN) channel, a coding error rate of not more than 10^{-5} . Since the 110C modulation mode does not contain 128QAM, according to the average of the SNR corresponding to 64QAM and 256QAM, the average SNR corresponding to 128QAM is 24dB. The average SNR for different modulation orders corresponding to the bit error rate $\leq 10^{-5}$ is shown in Table I.

The theoretical probability density function is obtained at the lower limit of the corresponding SNR, and the different mesh density and peak scale coefficients are obtained to get the binary feature matrix and clustered. Then find a balance between computational complexity and estimation performance and determine the value of $Meshnum$ and p .

IV. SNR ESTIMATION OF MQAM SIGNAL FOR SATELLITE-BASED IIOT

The constellation point coordinates after power normalization and quadratic coordinate correction are $r_{ad}(r_{iI}, r_{iQ})$, $i = 1, 2, \dots, L$. [26] is employed the M_2M_∞ method to estimate the SNR for the square constellation, which can be expressed as

$$\hat{\rho} \leftarrow LUT \left[\tilde{T}_\beta(r_{ad}) \right], \quad (29)$$

$$\begin{aligned} \tilde{T}_\beta(r_{ad}) = & \frac{E \left[R[r_{ad}(t)]^2 \right]}{(\max \{|R[r_{ad}(t)|]\} - \beta \min \{|R[r_{ad}(t)|]\})^2} \\ & + \frac{E \left[S[r_{ad}(t)]^2 \right]}{(\max \{|S[r_{ad}(t)|]\} - \beta \min \{|S[r_{ad}(t)|]\})^2}, \end{aligned} \quad (30)$$

where $R[\bullet]$ represents the real part, $S[\bullet]$ denotes the imaginary part, $\beta = s_{\max}/s_{\min}$ is the ratio of the modulus of the point where the modulus value is the largest in the constellation diagram and the point of the point where the modulus value is the smallest. $LUT[\bullet]$ denotes the look-up table method. The standard normalized constellation points

of 14 different constellation types are used to generate each entry of the table. The above SNR estimation method is suite for a square constellation. Since the constellation point of the square constellation does not fall on the coordinate axis, the denominator $\max\{|S[r_{ad}(t)]|\} - \beta \min\{|S[r_{ad}(t)]|\}$ of (30) can measure the degree to which the constellation is affected by noise. The outermost circle of the 110C circular constellation of 16/64QAM has four constellation points on the coordinate axis, so that $\min\{|S[r_{ad}(t)]|\}$ in the denominator tends to 0. Although $\tilde{T}_\beta(r_{ad})$ monotonically increases, but its increment is small and tends to be stable as the SNR increases.

When faced with 110C circular constellation of 16/64QAM, the SNR can be estimated with improved M_2M_∞ method as follows:

$$\hat{\rho} \leftarrow LUT \left[\tilde{T}_\beta(r_{ad}) \right], \quad (31)$$

$$\tilde{T}_\beta(r_{ad}) = \frac{E \left[R[r_{ad}(t)]^2 \right]}{(\max\{|R[r_{ad}(t)]|\} - \beta \min\{|R[r_{ad}'(t)]|\})^2} + \frac{E \left[S[r_{ad}(t)]^2 \right]}{(\max\{|S[r_{ad}(t)]|\} - \beta \min\{|S[r_{ad}'(t)]|\})^2}, \quad (32)$$

where $r_{ad}' = (r_{iI}', r_{iQ}')$ is the constellation points that satisfies

$$(r_{iI}', r_{iQ}') = \begin{cases} (r_{iI}, r_{iQ}), & \sqrt{r_{iI}^2 + r_{iQ}^2} < k_{pow} G_r, \\ k_{pow} (r_{iI}, r_{iQ}), & \sqrt{r_{iI}^2 + r_{iQ}^2} \geq k_{pow} G_r, \end{cases} \quad (33)$$

where $G_r = \max(\sqrt{r_{iI}^2 + r_{iQ}^2})$, k_{pow} is the pre-defined power coefficient, which should be greater than the ratio of the innermost constellation point power to the outermost constellation point power.

The square root normalized mean square error (SNMSE) of the SNR estimation for MQAM signal is [26]

$$SNMSE = \sqrt{\frac{1}{L} \sum_{i=1}^L \left(\frac{\hat{\rho}_i - \rho}{\rho} \right)^2}, \quad (34)$$

where $\hat{\rho}$ and ρ are estimation results and the real value of the estimated SNR. The normalized Cramer-Rao lower bound (CRLB) of the SNR estimation for MQAM signal is [28]

$$\frac{100}{L \ln^2(10)} \left(1 + \frac{2}{\rho} \right). \quad (35)$$

From the above analysis, the procedure of the introduced signal estimation method is summarized in Algorithm 1.

V. NUMERIC SIMULATION AND DISCUSSION

In this section, simulations and the corresponding analysis will be conducted to evaluate the performance of the proposed signla estimation methods. We take 50000 samples and 4QAM, 16QAM-square, 16QAM-110C circular, 16QAM-QCI circular, 32QAM-cross, 32QAM-110C circular, 32QAM-QCI circular, 64QAM-square, 64QAM-110C circular, 64QAM-QCI circular, 128QAM-cross, 256QAM-square, 256QAM-110C circular, 256QAM-QCI circular as a trial source, and

Algorithm 1 The procedure of signal estimation in CSNs for satellite-based IIoT.

- 1: For any received constellation point sequences, set the same p and $Meshnum$.
- 2: Estimate the continuous probability density function by (13).
- 3: Construct the binary real points by (19).
- 4: Estimate the modulation order and constellation type by (28).
- 5: If the constellation type is 110C circular of 16/64QAM, SNR is estimated by (31), (32) and (33), SNR of the else constellation type of MQAM can be estimated by (30).

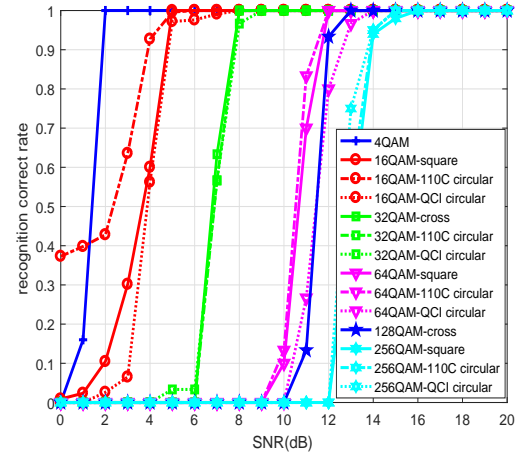


Fig. 2. Recognition correct rate of modulation parameters with different constellation types versus different SNRs

carry out a series of simulation experiments to assess the performance of the proposed signal estimation methods for satellite-based IIoT.

Table II shows the number of true points and the clustering result of the binary feature matrix of the 256QAM-QCI circular constellation, where the bold data is the case of successful recognition. In the case of the lower SNR corresponding to Table I, the different mesh density and peak-scale coefficients are taken. Taking the most complex 256QAM-QCI circular constellation in the signal set as an example, the theoretical probability density function is obtained under the condition of 27dB. Take a grid density from 10 to 100 in steps of 10 and take a peak scale factor from 0.1 to 0.9 in steps of 0.1 to obtain a binary feature matrix and cluster it. The five different clustering radii are $r_1 = 0.35$, $r_2 = 0.21$, $r_3 = 0.14$, $r_4 = 0.08$, $r_5 = 0.05$, respectively [29]. In order to balance the computational complexity and estimation performance, we set $Mushnum = 60$ and $p = 0.3$ in this paper.

Fig. 2 shows the recognition correct rate of modulation parameters with different constellation types versus different SNRs. The symbol rate of the signal is 1MBaud, the over-sampled rate is 8, the number of transmitted symbols is 5000, and the data multiplexing method is mirror mapping reuse. The roll-off factor of raised cosine roll-off filter is 0.5. Note that all the different signals on different constellation types

TABLE II
THE NUMBER OF TRUE POINTS OF 256QAM-QCI CIRCULAR CONSTELLATION BINARY VALUE MATRIX ($SNR=25dB$)

p \ $Meshnum$	10	20	30	40	50	60	70	80	90	100
0.1	20	68	164	256	456	544	812	1068	1352	1640
0.2	12	44	108	172	264	360	588	788	928	1156
0.3	12	36	76	128	192	304	400	620	640	872
0.4	12	36	76	112	164	264	288	448	504	668
0.5	4	16	36	76	88	172	228	308	368	428
0.6	4	12	36	40	52	148	176	176	280	324
0.7	4	12	36	40	24	132	132	124	240	244
0.8	4	12	20	32	16	76	72	72	152	168
0.9	4	12	12	20	12	44	44	52	80	116

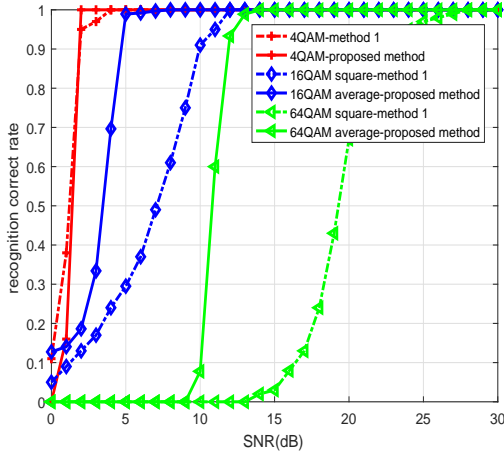


Fig. 3. Performance comparison between the proposed method and the method in [19] versus different SNRs

go through the same signal processing procedure, which is listed in Algorithm 1, and all the parameters are the same for all the modulation formats. From Fig. 2, it can be seen that the proposed estimation method could provide the best overall performance for different constellation types of MQAM signal. This method not only can estimate the modulation order, but also has good constellation type estimation performance for MQAM signal. The recognition rates of different constellation types under the same modulation order are basically similar, and the recognition rate decreases with the increase of the modulation order and SNR, which is consistent with the theory. The recognition SNR threshold (recognition correct rate $> 90\%$) of MQAM signal with different modulation orders and different constellation types are 4QAM (2dB), 16QAM (5dB), 32QAM (8dB), 64QAM (13dB), 128QAM (11dB), 256QAM (14dB), which meet the demodulation needs in Table I.

Fig. 3 is performance comparison between the proposed method and the method in [19] with different SNRs. Since the [19] method (method 1) is not universal, the signal set of the comparison method is limited to the 4QAM, 16QAM-square, 64QAM-square signal. In this paper, the recognition accuracy is greater than 90%, which means that this method is effective. From Fig. 3, it is seen that the 4QAM can achieve 100% recognition correct rate in method 1 when the ratio is greater than or equal to 2dB, which is the same as the

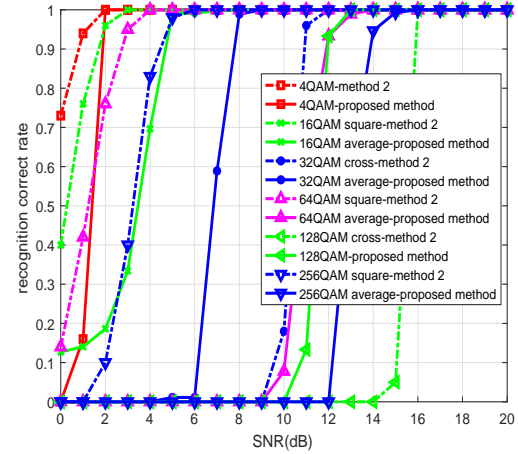


Fig. 4. Performance comparison between the proposed method and the method in [29] versus different SNRs

recognition threshold of the proposed method. The 16QAM is successfully identified at 10dB in method 1, which is higher than the 16QAM average recognition threshold (5dB) in the proposed method. The 64QAM is successfully identified at 22dB in method 1, which is higher than the 64QAM average recognition threshold (12dB) in the proposed method and higher than the 21dB demodulation threshold specified by the 110C military standard. The recognition correct rates of the proposed method and the method 1 decreases with the increase of the modulation order and increases with the increase of the SNR, which is consistent with the theory. Moreover, the method 1 is not universal, the method 1 will not suit for circular constellations in the MQAM signal.

Fig. 4 is performance comparison between the proposed method and the method in [29] with different SNRs. The comparison method is the method in [29]. Since the [29] method (method 2) is not universal, the signal set of the comparison method is limited to the 4QAM, 16QAM-square, 32QAM-cross, 64QAM-square, 128QAM-cross, 256QAM-square signal. From Fig. 4, it is seen that the 4QAM can achieve 100% recognition correct rate in method 2 when the ratio is greater than or equal to 1dB, which is similar to the identification threshold (2dB) of the proposed method. The method 2 of 16QAM-square constellation is successful at 2dB, which is slightly lower than the 16QAM average recognition threshold (5dB). The 64QAM-square constellation

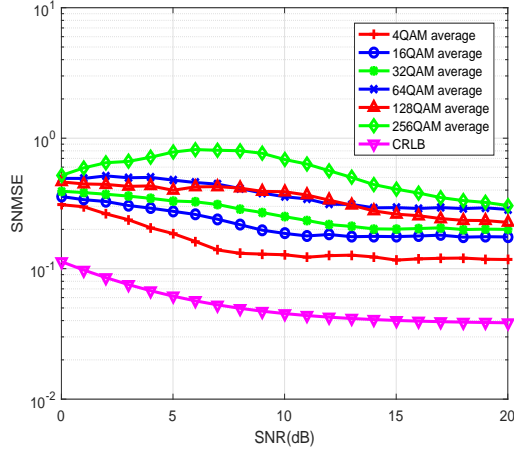


Fig. 5. SNMSE of improved M_2M_∞ method with different types of constellation

comparison method is successful at 3dB in method 2, which is lower than the 64QAM average recognition threshold (12dB). The comparison method of 256QAM-square constellation is successfully recognized at 5dB in method 2, which is lower than the average recognition threshold of 256QAM (14dB). However, for the cross constellation diagram, the recognition threshold of the method 2 is higher than the proposed method. The 32QAM-cross of method 2 is successfully identified at 11dB, which is higher than the 32QAM average recognition threshold (8dB). The 128QAM-Cross of method 2 is successfully identified at 16dB, which is higher than the 128QAM average recognition threshold (11dB). The recognition correct rate of the method 2 decreases with the increase of the modulation order and increases with the increase of the SNR. The recognition correct rate of the method 2 is related to the type of the constellation, in which the square is higher than the cross. When the type of the constellation is the same, the recognition correct rate decreases with the increase of the modulation order and increases with the increase of the SNR, which is consistent with the theory. Moreover, the method 2 is not universal, the method 2 will not suit for circular constellations in the MQAM signal.

Fig. 5 is the SNR estimation performance of the proposed method with different constellation types of MQAM signal. Since the monotonic feature $\tilde{T}_\beta(r_{ad})$ extracted in this paper is related to the length of the signal, when the table lookup table is created, the feature quantity is also calculated by using 500 symbols. The improved M_2M_∞ method is used to estimate SNR, and the SNMSE of the SNR estimation when SNR from 0 dB to 20 dB is shown in Fig.5. Fig. 5 shows that the distribution of constellation points in the 4QAM square constellation is simple and its SNMSE is closest to CRLB, which decreases from 0.32 to 0.12, and gradually stabilizes after 8dB. The estimated SNMSE of other constellation types of MQAM gradually moves away from CRLB as the modulation order increases but does not exceed 1. The sudden increase in SNMSE at high SNR in the SNR estimation method by using higher-order moments is eliminated. The average SNMSE of the three constellations of 16QAM decreased from 0.35 to

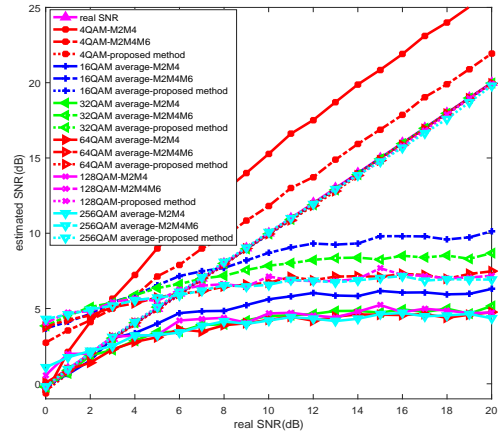


Fig. 6. SNR estimation performance comparison with different constellation types and modulation orders

0.19 and stabilized after 10dB. The average SNMSE of the three constellations of 32QAM decreased from 0.41 to 0.22, and gradually stabilized after 14dB. The average SNMSE of the three constellations of 64QAM dropped from 0.44 to 0.25 and stabilized after 18dB. The SNMSE of the 128QAM cross constellation map dropped from 0.45 to 0.23, and gradually stabilized after 18dB. The SNMSE of the cross constellation of 128QAM decreased from 0.45 to 0.23, and gradually stabilized after 18dB. The average SNMSE of the three constellations of 256QAM rises from 0.55 to 0.8, and then gradually decreases to around 0.3. That is, the SNMSE does not strictly decrease with the increase of the signal-to-noise ratio and shows an upward trend at 0-10dB. This means that within these ranges, the received signal is not highly dependent on the estimated parameters. That is, a small change in the SNR within a certain range does not cause a large change in the received signal at the receiving end, and the received signal does not bring a large amount of information about the SNR, therefore, the SNMSE also fluctuates. This phenomenon seems to be inherent to all constellations with non-constant modulus, as this is also the case in the estimation of other parameters of the MQAM signal, such as carrier frequency and carrier phase. It can be seen that no matter what type the constellation is, the improved M_2M_∞ method proposed in this paper can make the residual mean square error close to CRLB in the whole SNR interval. This proposed method solves the problem that the SNMSE of the conventional methods increase greatly in high SNR regions.

Fig. 6 is the SNR estimation performance comparison with different constellation types. The comparison method is the M_2M_4 and M_6 method. There are 14 different constellation types of MQAM signal, and the average value of the SNR estimated from 0 dB to 30 dB is shown in Fig. 6. From Fig. 6, it can be seen that the M_2M_4 and M_6 methods cannot accurately estimate the SNR of the 4QAM signal, but the trend is close to the actual SNR. When the signal is other MQAM signals, the M_2M_4 and M_6 methods cannot estimate the SNR because the constellation becomes more complicated. This is

because with the improvement of the SNR and the complexity of the constellation diagram, the statistics used to estimate the SNR tend to be stationary, and the proposed method based on improved M_2M_∞ is applicable to different constellation types and different modulation orders.

VI. CONCLUSION

In CSNs, MQAM signal estimation are very challenging, especially when no any priori information is available. In this paper, a novel non-data assisted MQAM signal estimation method is proposed for satellite-based IIoT, consisting of three main components, modulation order estimation, the constellation type estimation and SNR estimation. In the proposed method, the constellation diagram is obtained according to the baseband signal firstly. Then, the constellation diagram is processed by the grid method to estimate the probability density distribution function of constellation points. Secondly, set the peak scale factor and use the section to obtain the binary feature matrix of the probability density function. After that, the SNR estimation is carried out based on the improved M_2M_∞ and using the look-up table method according to the modulation order and the type of constellation. Finally, extensive simulation studies are conducted and the corresponding simulation results show that the recognition correct rate of modulation constellation types increases with the increase of the SNR and decreases with the increase of the modulation order. Apparently, it indicates that the proposed SNR estimation method could achieve excellent performance with different modulation orders and different constellation types.

REFERENCES

- [1] X. Liu, X. Zhai, W. Lu, and C. Wu, "QoS-guarantee resource allocation for multibeam satellite industrial internet of things with NOMA," *IEEE Transactions on Industrial Informatics*, DOI: 10.1109/TII.2019.2951728, Nov. 2019.
- [2] F. Li, K. Lam, N. Zhao, X. Liu, K. Zhao, and L. Wang, "Spectrum trading for satellite communication systems with dynamic bargaining," *IEEE Transactions on Communications*, vol. 66, no. 10, pp. 4680-4693, May 2018.
- [3] D. Hu, L. He, and J. Wu, "A novel forward-link multiplexed scheme in satellite-based internet of things," *IEEE Internet of Things Journal*, vol. 5, no. 2, pp. 1265-1274, Apr. 2018.
- [4] H. Song, X. Fang, L. Yan and Y. Fang, "Control/user plane decoupled architecture utilizing unlicensed bands in LTE systems," *IEEE Wireless Communications*, vol. 24, no. 5, pp. 132-142, Oct 2017.
- [5] X. Liu, M. Jia, X. Zhang, and W. Lu, "A novel multichannel internet of things based on dynamic spectrum sharing in 5G communication," *IEEE Internet of Things Journal*, vol. 6, no. 4, pp. 5962-5970, Aug. 2019.
- [6] V. Gouldieff, J. Palicot, and S. Daumont, "Blind modulation classification for cognitive satellite in the spectral coexistence context," *IEEE Transactions on Signal Processing*, vol. 65, no. 12, pp. 3204-3217, June 2017.
- [7] W. Zhang, F. Gao, S. Jin and H. Lin, "Frequency synchronization for uplink massive MIMO systems," *IEEE Transactions on Wireless Communications*, vol. 17, no. 1, pp. 235-249, Jan. 2018.
- [8] H. Song, X. Fang and C. Wang, "Cost-reliability tradeoff in licensed and unlicensed spectra interoperable networks with guaranteed user data rate requirements," *IEEE Journal on Selected Areas in Communications*, vol. 35, no. 1, pp. 200-214, Jan 2017.
- [9] X. Yan, K. An, T. Liang, G. Zheng, and Z. Feng, "Effect of imperfect channel estimation on the performance of cognitive satellite terrestrial networks," *IEEE Access*, vol. 7, pp. 126293-126304, Sep. 2019.
- [10] X. Zhang et al., "Outage Performance of NOMA-Based Cognitive Hybrid Satellite-Terrestrial Overlay Networks by Amplify-and-Forward Protocols," *IEEE Access*, vol. 7, pp. 85372-85381, 2019.
- [11] Digital video broadcasting (DVB) framing structure, channel coding and modulation for 11/12 GHz satellite services, ETSI EN300 421 V1.12, Aug. 1997.
- [12] European standard digital video broadcasting (DVB) second generation framing structure, channel coding and modulation systems for broadcasting, interactive services, news gathering and broadband satellite applications, ETSI EN 302 307 V1.1.1, Mar. 2013.
- [13] Q. Gao, G. Zhu, S. Lin, and C. Fu, "Variable-rate variable-power MQAM for spectral efficiency maximization in full-duplex systems," *IEEE Wireless Communications Letters*, vol. 7, no. 3, pp. 288-291, June 2018.
- [14] Interoperability and performance standards for data modems US military standard, MIL-STD-188-110C, Sep. 2011.
- [15] F. Kayhan, "QAM to circular isomorphic constellations," in *Proc. 2016 8th Advanced Satellite Multimedia Systems Conference and the 14th Signal Processing for Space Communications Workshop*, Palma de Mallorca, Oct. 2016, pp. 1-5.
- [16] M. Liu, G. Liao, Z. Yang, H. Song, and F. Gong, "Electromagnetic signal classification based on deep sparse capsule networks," *IEEE Access*, vol. 7, pp. 83974-83983, June. 2019.
- [17] J. Wang, B. Li, M. Liu, and J. Li, "SNR estimation of time-frequency overlapped signals for underlay cognitive radio," *IEEE Communications Letters*, vol. 19, no. 11, pp. 1925-1928, Sep. 2015.
- [18] M. Liu, L. Liu, H. Song, Y. Hu, Y. Yi, and F. Gong, "Signal estimation in underlay cognitive networks for industrial internet of Things," *IEEE Transactions on Industrial Informatics*, DOI: 10.1109/TII.2019.2952413, Nov. 2019.
- [19] H. Abuella, and M. Ozdemir, "Automatic modulation classification based on kernel density estimation," *Canadian Journal of Electrical and Computer Engineering*, Vol. 39, no.3, pp. 203-209, July 2016.
- [20] M. Laghate, S. Chaudhari and D. Cabric, "USRP N210 demonstration of wideband sensing and blind hierarchical modulation classification," in *Proc. 2017 IEEE International Symposium on Dynamic Spectrum Access Networks*, Piscataway, NJ, May 2017, pp. 1-3.
- [21] Y. Zhao, X. Yang and Y. Lin, "A new recognition method for MQAM signals in software defined radio," in *Proc. 2017 IEEE International Conference on Software Quality, Reliability and Security Companion*, Prague, Aug. 2017, pp. 271-275.
- [22] H. Ren, J. Yu, Z. Wang, J. Chen and C. Yu, "Modulation format recognition in visible light communications based on higher order statistics," in *Proc. 2017 Conference on Lasers and Electro-Optics Pacific Rim*, Singapore, Nov. 2017, pp. 1-2.
- [23] Y. Kumar, G. Jajoo, and S. Yadav, "Modulation scheme detection of blind signal using constellation graphical representation," in *Proc. 2017 International Conference on Computer, Communications and Electronics*, Jaipur, Aug. 2017, pp. 231-235.
- [24] J. Tian, T. Zhou, T. Xu, H. Hu and M. Li, "Blind estimation of channel order and SNR for OFDM systems," *IEEE Access*, vol. 6, pp. 12656-12664, Jan. 2018.
- [25] X. Qun and Z. Jian, "Improved SNR estimation algorithm," in *Proc. 2017 International Conference on Computer Systems, Electronics and Control*, Dalian, Aug. 2017, pp. 1458-1461.
- [26] S. Khalid and S. Abrar, "A non-data-aided SNR estimation method for square-QAM system," in *Proc. 2013 11th International Conference on Frontiers of Information Technology*, Islamabad, Jan. 2013, pp. 146-149.
- [27] Y. Zhao, W. Li, B. Yang and X. Mao, "Modified method of input SNR estimation for robust adaptive beamforming," in *Proc. 2017 International Applied Computational Electromagnetics Society Symposium*, Suzhou, Sep. 2017, pp. 1-2.
- [28] F. Bellili, A. Sthepenne, and S. Affes, "Cramer-Rao lower bounds for NDA SNR estimates of square QAM modulated transmissions," *IEEE Transactions on Communications*, vol. 58, no. 11, pp. 3211 - 3218, Dec. 2010.
- [29] L. Wang and Y. Li, "Constellation based signal modulation recognition for MQAM," in *Proc. 2017 IEEE 9th International Conference on Communication Software and Networks*, Guangzhou, Dec. 2017, pp. 826-829.